



Journal Name

SUPPORTING INFO

Determination of quantum yields of semiconductor nanocrystals at single emitter level via fluorescence correlation spectroscopy.

Gerardo Abbandonato ^{a,b}, Katrin Hoffmann ^a, Ute Resch-Genger ^{a,*}

a. Federal Institute for Materials Research and Testing (BAM), Division *Biophotonics*, Richard-Willstaetter-Str. 11, 12489 Berlin, Germany.

b. NEST, Scuola Normale Superiore and NANO-CNR, Piazza San Silvestro 12, 56127 Pisa, Italy.

Corresponding Author

Ute Resch-Genger

Federal Institute for Materials Research and Testing (BAM),

Richard-Willstaetter-Str. 11, 12489 Berlin, Germany.

E-mail: ute.resch@bam.de

KEYWORDS. semiconductor nanocrystal, quantum dot, quantum yield, molecular brightness, fluorescence correlation spectroscopy FCS, single molecule

Contents

1 - Detailed fitting procedure of FCS-based measurements used for the determination of the photoluminescence (PL) quantum yield (Φ_f) of fluorescent dyes and QDs.....	2
2 - Effect of QD concentration on Φ_f and PL lifetime measurements.....	6

1. Detailed fitting procedure of FCS-based measurements used for the determination of the photoluminescence (PL) quantum yield (Φ_F) of fluorescent dyes and QDs

As reported by Kempe et al.¹, the count rate per molecule per unit time or molecular brightness MB, was obtained from the ratio between the average count rate $\langle I \rangle$ and the average number of particles $\langle N \rangle$. The average count rate $\langle I \rangle$ equals the mean value of the binned fluorescence intensity trace (Figure S1). The influence on the background on the intensity mean values was negligible with respect to the size of the measured intensity signal. Measurements of the pure solvent with the same excitation intensity as used for the samples gave a very low detector noise for the used single-photon avalanche diode ($\mu = 0.44$, $\sigma = 0.676$).

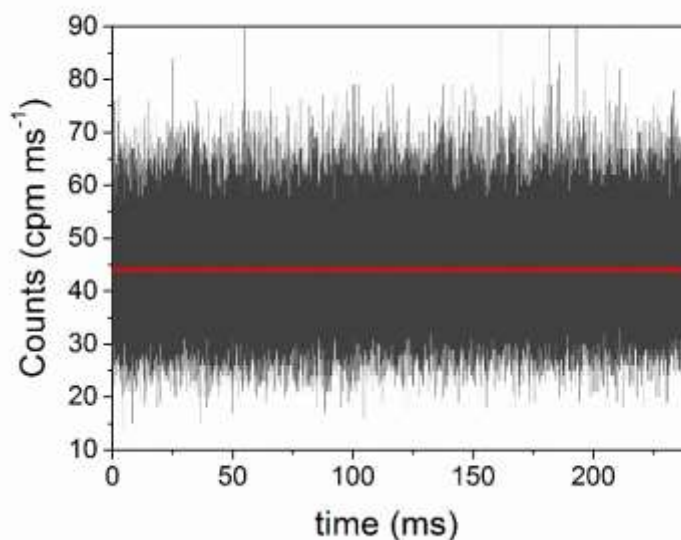


Figure S1. Time trace obtained during the measurement of the QD sample QDR, a red emitting CdTe colloid. The mean fluorescence count-rate $\langle I \rangle$ is shown in red.

The number of particles $\langle N \rangle$ was derived by fitting the autocorrelation function (ACF). The autocorrelation function (ACF) of $G(\tau) = \langle I(t)I(t + \tau) \rangle_t$ of the intensity trace $I(t)$ represents the probability to find the same signal at the time delayed by τ .

The ACF due to free 3D translational diffusion of a point-like particle is given in equation S1.

$$G(\tau) = G(0) \left(1 + \frac{\tau}{\tau_D}\right)^{-1} \left(1 + \left(\frac{\omega_{xy}}{\omega_z}\right) \frac{\tau}{\tau_D}\right)^{-0.5} \quad (\text{eq. S1})$$

Here ω_{xy} and ω_z are the equatorial and axial waist of the observation volume, respectively, which is mathematically described by a 3D Gaussian function.² The amplitude $G(0)$ of ACF gives the reciprocal of the average number of the fluorescent particles $G(0) = 1/\langle N \rangle$ crossing the observation volume during data acquisition, while the characteristic time of the fluctuation τ_D is related to the diffusion coefficient (D) by $\tau_D = \omega_{xy}^2/4D$.³ The Stokes-Einstein equation provides the relationship between D and the hydrodynamic radius (R_H) of a spherical emitter $D = k_B T / 6\pi\eta R_H$, where k_B is the Boltzmann constant, η the medium's viscosity, and T the temperature, respectively.

When the emitter (like molecular dyes, Figure S2a) undergoes significant dark states (i.e. triplet state), the ACF needs to be modified by introducing a multiplicative term accounting for this further fluctuation of the emission intensity. In this perspective, the eq. S1 is modified as follows

$$G(\tau) = G(0) \left(1 + \frac{T}{1-T} \exp\left(-\frac{\tau}{\tau_T}\right)\right) \left(1 + \frac{\tau}{\tau_D}\right)^{-1} \left(1 + \left(\frac{\omega_{xy}}{\omega_z}\right) \frac{\tau}{\tau_D}\right)^{-0.5} \quad (\text{eq. S2})$$

Here, T denotes the fraction of the particles in the dark triplet state with the characteristic triplet time τ_T .

The characteristic QD blinking can be observed on a broad time scale from 200 μs to 10 s. Because of its stochastic nature, it is not straightforwardly parameterizable as a “dark state” in the ACF. In our case all the curves deriving from QDs measurements could be fitted with eq. S1 for free 3D translational diffusion (Figure S2b).

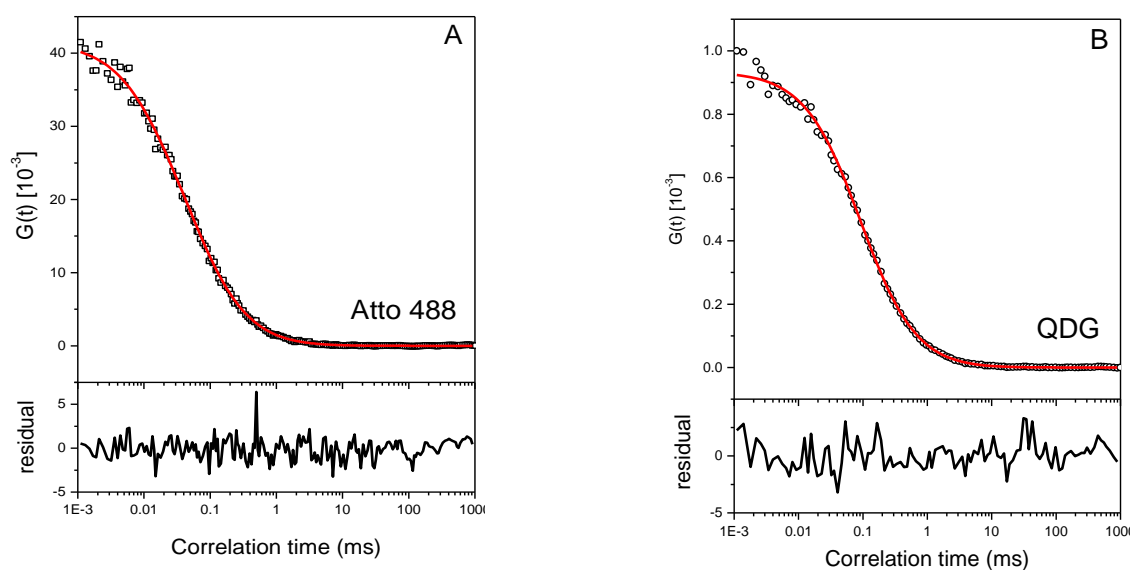


Figure S2. (A) Autocorrelation-curve of Atto 488 in 0.1 M PBS analyzed with eq. S2. (B) Autocorrelation curve of QDG in water analyzed with eq. S1. In both the cases, the fitted model curve is given in red and the residues are depicted under the curves.

The determination of the observation volume and the aspect ratio (that is ω_{xy} and ω_z), the absolute values of the diffusion coefficients of Atto 488-carboxylic acid in PBS (400 $\mu\text{m}^2/\text{s}$, 25°C), Fluorescein in water containing 0.1 M NaOH (425 $\mu\text{m}^2/\text{s}$, 25°C), and Alexa 647 in PBS (330 $\mu\text{m}^2/\text{s}$, 25°C), using the values reported by PicoQuant GmbH⁴, were fixed as calibration values.

After the FCS analysis, the following calculations were accomplished for the Φ_F determination. Initially the calculation of the MB values for each LP .

$$MB = \langle I \rangle / \langle N \rangle \quad (\text{eq. S3})$$

The trend of MB vs. laser power (LP) was analyzed using two different model functions. For the molecular fluorophores, we assumed a linear relationship in the “low” regime power and just hence the corresponding linear fit.

$$MB = m \cdot LP \quad (\text{eq. S4})$$

For QDs, we employed a function similarly to the saturation equation (see eq. 5 in the manuscript (ms))

$$MB = MB_0 \frac{LP}{LP + LP_S} \quad (\text{eq. S5})$$

The determination of the slope m for LP approaching zero (zero limit LP) was performed using the limit of the derivate of equation (eq. S5)

$$\lim_{LP \rightarrow 0} \frac{d(MB)}{d(LP)} = \frac{MB_0}{LP_S} = m \quad (\text{eq. S6})$$

Then, eq. 2 in the ms was used to finally calculate Φ_F .

In a first step, we determined Φ_F of Fluorescein in 0.1M NaOH/water in order to validate the microscopic method from Kempe et al.¹ and to test our experimental set-up. As reference dye we used Atto 488 (in PBS), known to show a high Φ_F and to undergo very little triplet formation.⁵

Comparison of the slopes of the FCS-derived data of these two dyes yielded a Φ_F value of 0.87 ± 0.04 for Fluorescein in 0.1M NaOH/water. The result slightly differs from reported values (0.87⁶, 0.89⁷, 0.91⁸, 0.81⁹) by 4-7% which is in the order of the generally accepted uncertainty of 5-10 % of Φ_F determination with commonly used optical methods.⁷

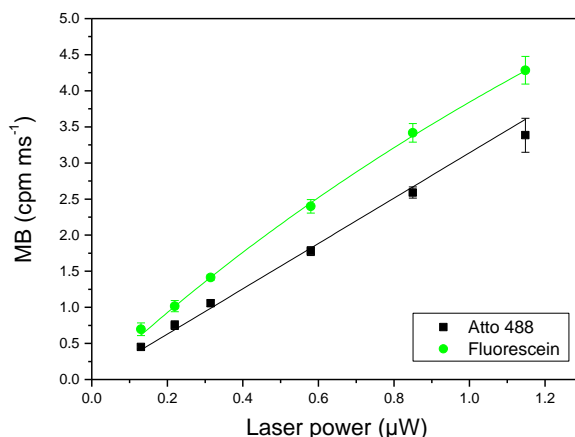


Figure S3. MB plot for Fluorescein (green circles) and the reference dye Atto 488 (black squares).

Fluorescein suffers from a low photostability and reveals a high photobleaching rate¹⁰. It exhibited a significant deviation from the required linearity between MB and LP , in contrast to rather photostable Atto 488. For this reason, the MB vs. LP plot was analyzed with the saturation-like eq. S5 instead of the linear equation eq. S4 valid for stable fluorophores.

Table S1 summarizes all parameters relevant for the determination of Φ_F with the microscopy method. The integrated transmission parameter g is a correction factor accounting for all optical elements in the light path and the quantum efficiency of the detector and is hence specific for the used microscope. g was determined experimentally by equation S7 according to the procedure reported by Kempe et al.¹.

$$g = \int_{\lambda} Em(\lambda) \cdot g(\lambda) d\lambda \quad (\text{eq. S7})$$

Here, $Em(\lambda)$ is the integral-normalized fluorescence emission spectra and $g(\lambda)$ is the function describing the optical elements in the light path (i.e. dichroic mirrors, acquisition filter transmittance). The functions $Em(\lambda)g(\lambda)$, which were experimentally determined for each analyzed organic fluorophore or QD, are presented in Figure S4.

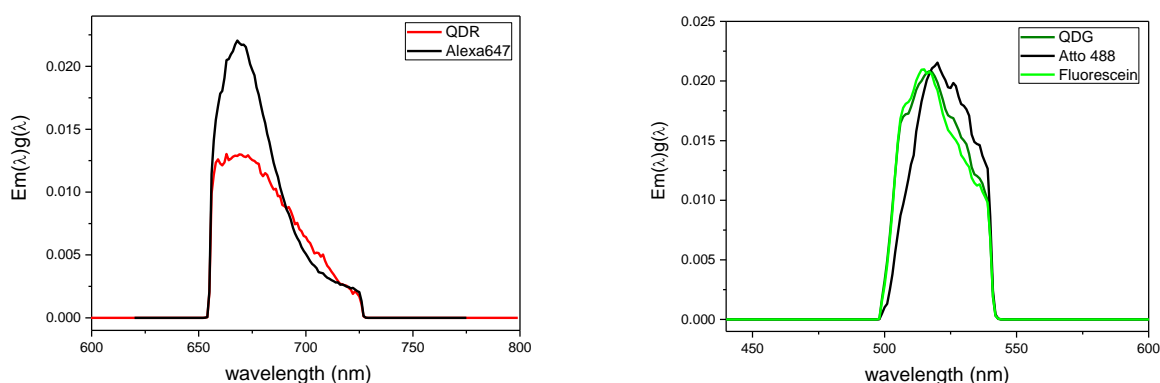


Figure S4. Experimental transmission functions $Em(\lambda)g(\lambda)$ (eq. S7) of the analyzed fluorophores and QDs, respectively.

Table S1. Compilation of the spectroscopic data of the organic fluorophores, QDG, and QDR and all parameters relevant for the determination of Φ_f by means of the microscopy-based method. $\langle\epsilon(\lambda_{ex})\rangle$ denotes for the integral extinction along the excitation profile of the exciting laser centered at 485 nm and 640 nm, respectively. g is the instrument-specific correction factor and m the slope derived from the MB plots, respectively.

Fluorophore	λ_{abs}	λ_{em}	$\epsilon(\lambda_{ex})$	$\langle\epsilon(\lambda_{ex})\rangle$	g	m
	nm	nm	$M^{-1}cm^{-1}$	$M^{-1}cm^{-1}$		$cpm\ ms^{-1}\mu W^{-1}$
Atto 488	500	520	90,000	49,394	0.605	3.141
Fluorescein	490	519	93,000	69,712	0.612	4.881
QDG	485	520	45,528	45,256	0.627	6.961
Alexa 647	650	665	270,000	192,321	0.746	2.261
QDR	620	660	175,000	153,368	0.582	2.875

2. Effect of QD concentration on Φ_F and PL lifetime measurements

Three different concentrations were evaluated for QDG and QDR. From the measured data and fitted ACF functions, the QD concentrations were calculated to ~ 72 nM, ~ 142 nM, and ~ 284 nM for QDG and ~ 31 nM, ~ 62 nM, and ~ 124 nM for QDR, respectively (see Figure S5a-d).

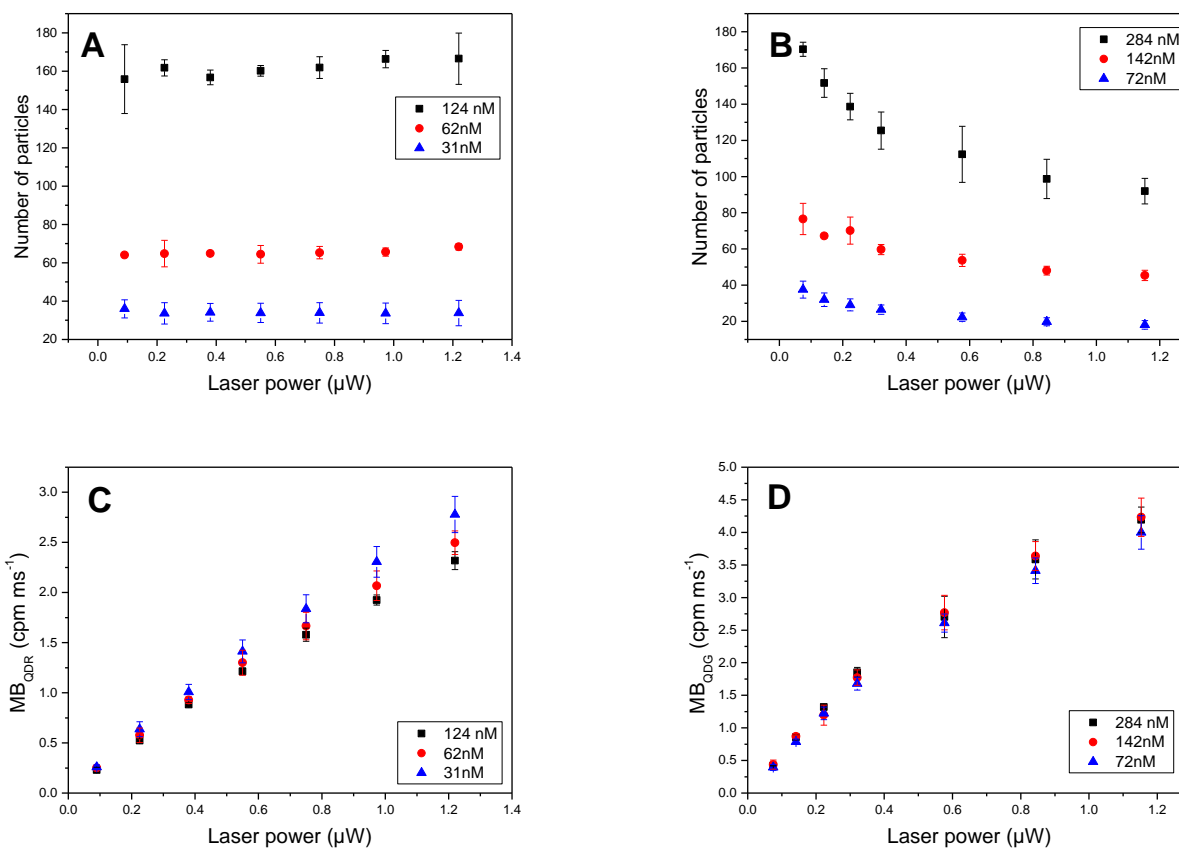


Figure S5. Evaluation of the data derived from the ACF function of the QDs for the different QD concentrations. Number of particles of QDR (A) and QDG (B). MP vs. LP plots for different concentrations of QDR (C) and QDG (D).

Table S2. Φ_F data calculated from MP vs. LP plots (Figure S5, panels C and D) for different concentrations of QDR and QDG.

QDG		QDR	
Conc (nM)	PL QY	Conc (nM)	PL QY
284	0.348 \pm 0.020	124	0.596 \pm 0.015
142	0.340 \pm 0.038	62	0.700 \pm 0.138
72	0.316 \pm 0.027	31	0.675 \pm 0.065

In the case of QDR, the lifetime analysis given in Figure S6A revealed no significant dependence on QD concentration and LP ; this is in excellent agreement with the general behavior of blinking and saturation recorded from the ACF and with the result of the MB . For this CdTe colloid, no concentration-dependent changes in Φ_F have been observed. Φ_F of the smaller CdTe QD QDG, however, showed a slight decrease of Φ_F with the colloid concentration. This seems to reflect the behavior observed previously for other CdTe colloids, where smaller QDs were more prone to ligand desorption-induced fluorescence and Φ_F reduction than larger ones⁶. The PL lifetime measurements confirmed these findings. The lifetime vs. LP plot for QDG (Figure 6B) revealed the same dependence on LP (the higher LP , the shorter the PL lifetime) and a dependence on nanocrystal concentration (the smaller the QD concentration, the shorter the PL lifetime) in agreement with the calculated Φ_F .

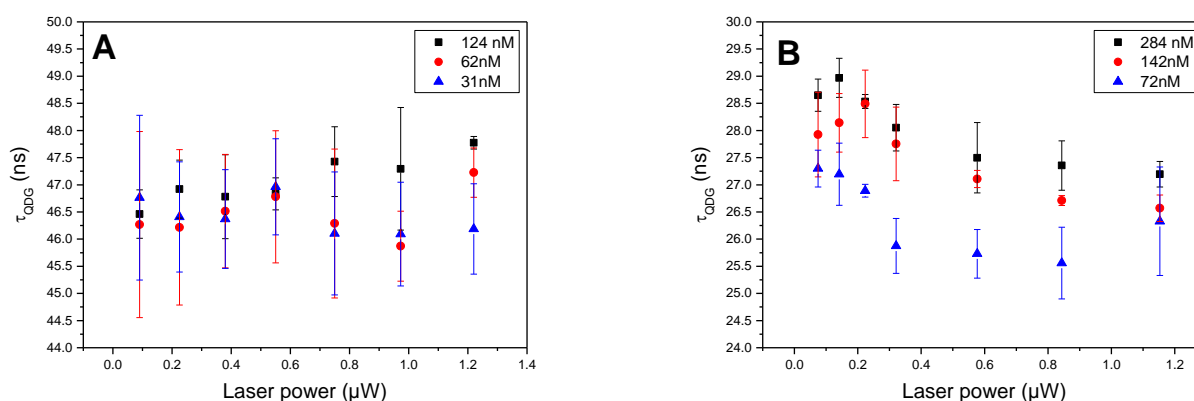


Figure S6. PL lifetime vs. LP plot for the different concentrations of QDR (A) and QDG (B) analyzed.

References

- (1) Kempe, D.; Schöne, A.; Fitter, J.; Gabba, M. *The Journal of Physical Chemistry B* 2015, *119*, 4668-4672.
- (2) Zhang, B.; Zerubia, J.; Olivo-Marin, J.-C. *Applied Optics* 2007, *46*, 1819.
- (3) Digman, M. A.; Gratton, E. *Annual Review of Physical Chemistry* 2011, *62*, 645-668.
- (4) Kapusta, P. Application Note Picoquant GmbH 2010.
- (5) https://www.atto-tec.com/attotecshop/product_info.php?language=en&info=p99_ATTO-488.html.
- (6) Grabolle, M.; Speiles, M.; Lesnyak, V.; Gaponik, N.; Eychmüller, A.; Resch-Genger, U. *Analytical Chemistry* 2009, *81*, 6285-6294.
- (7) Würth, C.; Grabolle, M.; Pauli, J.; Speiles, M.; Resch-Genger, U. *Nature Protocols* 2013, *8*, 1535-1550.
- (8) Cheknlyuk, A.; Fadeev, V.; Georgiev, G.; Kalkanjev, T.; Nickolov, Z. *Spectroscopy Letters* 2006, *15*, 355-365.
- (9) Magde, D.; Wong, R.; Seybold, P. G. *Photochemistry and Photobiology* 2007, *75*, 327-334.
- (10) Song, L.; Hennink, E. J.; Young, I. T.; Tanke, H. J. *Biophysical Journal* 1995, *68*, 2588-2600.